No. 561 February 2017

Thermal Maragoni Convection of Two-phase Dusty Fluid Flow Along a Vertical Wavy Surface

S. Siddiqa, N. Begum,
M. A. Hossain, R. S. R. Gorla

ISSN: 2190-1767

Thermal Maragoni Convection of Two-phase Dusty Fluid Flow Along a Vertical Wavy Surface

Sadia Siddiqa[*,1], Naheed Begum[♭], M. A. Hossain[§], Rama Subba Reddy Gorla[‡]

[*] *Department of Mathematics, COMSATS Institute of Information Technology, Kamra Road, Attock, Pakistan*

[♭] *Institute of Applied Mathematics (LSIII), TU Dortmund, Vogelpothsweg 87, D-44227 Dortmund, Germany*

[§] *UGC Professor, Department of Mathematics, University of Dhaka, Bangladesh*

[‡] *Department of Mechanical & Civil Engineering, Purdue University Northwest, Westville, Indiana 46391 USA*

Abstract: The paper considers the influence of thermal Maragoni convection on boundary layer flow of two-phase dusty fluid along a vertical wavy surface. The dimensionless boundary layer equations for two-phase problem are reduced to a convenient form by primitive variable transformation (PVF) and then integrated numerically by employing the implicit finite difference method along with the Thomas Algorithm. The effect of thermal Maragoni convection, dusty water and sinusoidal waveform are discussed in detail in terms of local heat transfer rate, skin friction coefficient, velocity and temperature distributions. This investigation reveals the fact that the water-particle mixture reduces the rate of heat transfer, significantly.

1 Introduction

Surface-tension-driven convection occurs when there is temperature or concentration differences on the surface of the fluid and the fluid will flow from region having low surface tension (high temperature region) to region having high surface tension (cold temperature region). In thermocapillary convection, the surface tension varies with temperature. However, small amounts of certain surfactant additives are also known to drastically change the surface tension. Surface-tension induced convection is of significant importance because it causes undesirable effects in industrial processes. The class of problems having surface-tension-driven convection or also known as Marangoni convection, is of prime importance in industrial, biomedical and daily life applications such as coating flow technology, microfluidics, surfactant replacement therapy for neonatal infants, film drainage in emulsions and foams, drying of semi-conductor wafers in microelectronics and in numerous fields of micro-gravity sciences and space processing. Napolitano ([1]-[2]) was the first who observed the existence of such dissipative layers that can be formed along the interface of two immiscible fluids, in surface driven flows. With the advancement of space experimentation under microgravity conditions, the Marangoni effect has attracted much attention. There was an expectation that heat convection in molten systems would disappear completely under microgravity conditions and that high quality crystals could thus be obtained as a consequence (for details see Ref. [1]). Marangoni (thermocapillary) convection may also arise in laser melt pools during epitaxial laser metal forming [3]. With mass transfer present also, solutal Marangoni convection arises wherein the flow is caused by surface tension gradients originating from concentration gradients. Thermocapillarity is flow caused by surface

[1]Corresponding Authors.
Email: saadiasiddiqa@gmail.com

tension gradients originating from temperature gradients. Studies of these problems are also motivated by their importance in terrestrial materials processing, and oceanography [4]. Batishchev [5] discussed Marangoni boundary layer degeneration at the outer boundary and the generation of a counter stream zone, also considering convective flows with directed crystallization, in the absence of mass forces. Napolitano and Russo [6] identified similarity solutions for Marangoni boundary layers arising for the case where interface temperature gradient varies as a power of the interface arc length. The significance of dissipative layers in liquid metal and semiconductor processing is shown to be particularly strong and is a major factor in guiding the control of industrial processes. However, although extensive work has been done in investigating the Marangoni convection, the state of the art is still somewhat unsatisfactory in what concerns preliminary questions of general and basic nature. In this context, it was proved by Napolitano [7] that, similar to that of classical boundary layers (also knows as non-Marangoni layers), while using the arc length x and the distance normal to the interface as coordinates, the field equations in the bulk fluids do not depend explicitly on the geometry of the interface. This includes, however, the average curvature of its hydrostatic and dynamic shapes and produces the kinematic, thermal and pressure couplings for the flow fields of two fluids. Afterwards, it was shown in [8] that, such coupling of the fields may be removed, when i) the viscosity ratio of the two fluids, and ii) the momentum and thermal resistivity ratios of the two layers, are strictly less than unity. The authors in [8] reported some interesting facts about Marangoni boundary layers, and proved that the existence of similar solutions for the class of Marangoni convection problems is only possible if temperature gradient at the surface varies as a power of arc length of the geometry. Besides, Christopher and Wang [9] have examined the effect of Prandtl number to see the relative thickness of momentum and thermal boundary layers. Furthermore, the detailed numerical as well as analytical solutions for Marangoni boundary layers were discussed by several authors under various practical situations (For details see [10]-[15]).

In all above-mentioned studies, attention has been given to viscous fluid which is free from all impurities (clear fluid). But, pure fluid is rarely available in many practical situations, for instance, common fluids like air and water contain impurities like dust particles. Therefore, investigations on flow of fluids with suspended particles have attracted the attention of numerous researchers due to their practical applications in various problem of atmospheric, engineering and physiological fields (see [16]). In this regard, Farbar and Morley [17] were the first to analyze the gas-particulate suspension on experimental grounds. After that, Marble [18] studied the problem of dynamics of a gas containing small solid particles and developed the equations for gas-particle flow systems. Singleton [19] was the first to study the boundary layer analysis for dusty fluid and later on several attempts were made to conclude the physical insight of such two-phase flows (see Ref. [20]-[25]) under different physical circumstances.

It is noteworthy to mention that the irregular surfaces, say, vertical or horizontal wavy surfaces have been considered vastly in the literature (see Ref. [26]-[31]). Through these analysis, it has been reported that such surfaces serves practically in engineering applications (for instance in solar collectors, grain storage containers, industrial heat exchangers and condensers in refrigerators). Motivated by the previous works and possible applications, thermal Maragoni convection of two-phase dusty fluid is modeled along a vertical wavy surface in the present study. From the present analysis we will interrogate whether i) the

roughness element and ii) the presence of dust particles in base fluid affect the Marangoni natural convection and alter the physical characteristics associates with the vertical wall or not? The upcoming section contains the elementary field equations of fluid mechanics as partial differential equations in terms of physically important unknown parameters such as velocity, pressure and energy variable for two-phase dusty fluid. To study the effects of surface-tension-driven convection, it is assumed that the temperature gradients for both phases at the wavy surface are in the form of power law function. In addition, dusty fluid flow equations are developed by considering the assumption made by Marble in [18]. The governing equations for two-phase model are then transformed into dimensionless boundary layer equations by incorporating a set of suitable transformations. After that, coordinate transformation (primitive variable formulation) is employed to transform the two-phase boundary layer model into a convenient form, which are solved numerically by hiring an implicit finite difference method along with the Thomas Algorithm (For details see Ref. [32]). Afterwards, results and discssion section is given, in which, computational data is presented graphically in the form of skin friction coefficient, heat transfer rate, velocity and temperature profiles, streamlines and isotherms by varying several controlling parameters. A tabular comparison of wall skin friction and rate of heat transfer for pure and dusty fluid is also given in the result and discussion section. Besides, the effect of Maragoni convection parameter, dust particle loading parameter and surface waviness parameter are taken into account and presented graphically. Lastly, important results from the present analysis are summarized in the conclusion section. We believe that the present results are a new addition to the open literature on thermal Maragoni convection in dusty fluids.

2 Mathematical Formulation

Considerations have been given to steady coupled problem of thermal Marangoni natural convection along an isothermal vertical wavy surface, as shown in Fig. 1. The shape of the wavy surface, $\sigma(\bar{x})$, is arbitrary, but our detailed numerical work will assume that the surface exhibits sinusoidal deformations. Thus, the wavy pattern of the vertical surface is described by:

$$\bar{y}_w = \sigma(\bar{x}) = \bar{a}\sin\left(\frac{2\pi\bar{x}}{L}\right) \tag{1}$$

where $\bar{a}$ is the dimensional amplitude of the wavy surface and L the characteristic length associated with the uneven surface. The working fluid is taken to be viscous, dusty and incompressible, which is originally at rest along a vertical heated wavy surface. Initially, the system is having a uniform temperature T_∞. Suddenly, the surface of the vertical plate at $\bar{y} = 0$ is heated to a temperature $T + \Delta T$ and natural convection starts due to this. The temperature gradients for both phases are in the form of power law function. Under the assumptions of the dusty fluid flow given in (For details see Ref. [21], [22]), the governing system of equations is developed as:
For gas phase:

$$\frac{\partial\bar{u}}{\partial\bar{x}} + \frac{\partial\bar{v}}{\partial\bar{y}} = 0 \tag{2}$$

$$\bar{u}\frac{\partial\bar{u}}{\partial\bar{x}} + \bar{v}\frac{\partial\bar{u}}{\partial\bar{y}} = -\frac{1}{\rho}\frac{\partial\bar{p}}{\partial\bar{x}} + \nu\nabla^2\bar{u} + g\beta_T(T - T_\infty) + \frac{\rho_p}{\rho\tau_m}(\bar{u}_p - \bar{u}) \tag{3}$$

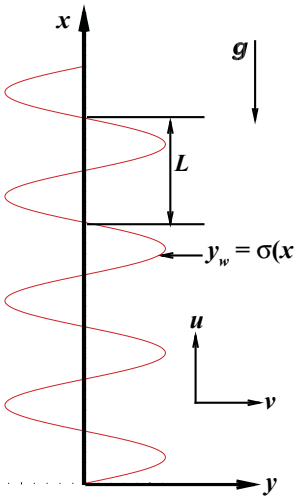

Fig. 1 The physical model.

$$\bar{u}\frac{\partial \bar{v}}{\partial \bar{x}} + \bar{v}\frac{\partial \bar{v}}{\partial \bar{y}} = -\frac{1}{\rho}\frac{\partial \bar{p}}{\partial \bar{y}} + \nu\nabla^2\bar{v} + \frac{\rho_p}{\rho\tau_m}(\bar{v}_p - \bar{v}) \tag{4}$$

$$\bar{u}\frac{\partial T}{\partial \bar{x}} + \bar{v}\frac{\partial T}{\partial \bar{y}} = \alpha\nabla^2 T + \frac{\rho_p c_s}{\tau_T \rho c_p}(T_p - T) \tag{5}$$

For the particle phase:

$$\frac{\partial \bar{u}_p}{\partial \bar{x}} + \frac{\partial \bar{v}_p}{\partial \bar{y}} = 0 \tag{6}$$

$$\rho_p\left(\bar{u}_p\frac{\partial \bar{u}_p}{\partial \bar{x}} + \bar{v}_p\frac{\partial \bar{u}_p}{\partial \bar{y}}\right) = -\frac{\partial \bar{p}_p}{\partial \bar{x}} - \frac{\rho_p}{\tau_m}(\bar{u}_p - \bar{u}) \tag{7}$$

$$\rho_p\left(\bar{u}_p\frac{\partial \bar{v}_p}{\partial \bar{x}} + \bar{v}_p\frac{\partial \bar{v}_p}{\partial \bar{y}}\right) = -\frac{\partial \bar{p}_p}{\partial \bar{y}} - \frac{\rho_p}{\tau_m}(\bar{v}_p - \bar{v}) \tag{8}$$

$$\rho_p c_s\left(\bar{u}_p\frac{\partial T_p}{\partial \bar{x}} + \bar{v}_p\frac{\partial T_p}{\partial \bar{y}}\right) = -\frac{\rho_p c_s}{\tau_T}(T_p - T) \tag{9}$$

where $(\bar{u}, \bar{v})$, T, ρ, c_p, β_T α, μ are respectively the velocity vector in the $(\bar{x}, \bar{y})$ direction, temperature, density, specific heat at constant pressure, volumetric expansion coefficient, thermal diffusivity and kinematic viscosity of carrier fluid. Similarly, $(\bar{u}_p, \bar{v}_p)$, T_p, ρ_p and c_s corresponds to the velocity vector, temperature, density and specific heat for the particle phase. In addition, g is the gravitational acceleration, τ_m (τ_T) is the momentum relaxation time (thermal relaxation time) for dust particles.

The fundamental equations stated above are to be solved under appropriate boundary conditions to determine the flow fields of the fluid and the dust particles. Therefore, the boundary conditions for the problem under considerations are:

For gas phase:

$$\begin{gathered}\mu\frac{\partial \bar{u}}{\partial \bar{y}}(\bar{x}, \bar{y}_w) = \hbar_T\frac{\partial T}{\partial \bar{x}}(\bar{x}, \bar{y}_w), \bar{v}(\bar{x}, \bar{y}_w) = 0, \\ T(\bar{x}, \bar{y}_w) - T_\infty = T_0, \bar{u}(\bar{x}, \infty) = 0, T(\bar{x}, \infty) = T_\infty.\end{gathered} \tag{10}$$

For particle phase:

$$\begin{array}{c}\mu\frac{\partial\bar{u}_p}{\partial\bar{y}}(\bar{x},\bar{y}_w)=\hbar_T\frac{\partial T_p}{\partial\bar{x}}(\bar{x},\bar{y}_w),\bar{v}_p(\bar{x},\bar{y}_w)=0,\\ T_p(\bar{x},\bar{y}_w)-T_\infty=T_0,\bar{u}_p(\bar{x},\infty)=0,T_p(\bar{x},\infty)=T_\infty.\end{array}\tag{11}$$

Here, $\hbar_T=-\frac{\partial\hbar}{\partial\bar{x}}$, where $\hbar$ is the surface tension which is assumed to be given by the linear relation:

$$\hbar=\hbar_m-\hbar_T(T-T_\infty)\tag{12}$$

where $\hbar_m$ is the surface tension at a reference temperature T_∞ and assumed to be constant. In order to transform all the above-mentioned quantities in Eqs. (1)-(12) in uniform order of magnitude, the following continuous dimensionless variables have been employed:

$$\begin{array}{l}x=\frac{\bar{x}}{L},\ y=\frac{\bar{y}-\sigma(\bar{x})}{L}Gr_L^{1/4},\ (\theta,\theta_p)=\frac{(T,T_p)-T_\infty}{T_0}\\ (u,u_p)=\frac{\rho L}{\mu}Gr_L^{-1/2}(\bar{u},\bar{u}_p),\ (p,p_p)=\frac{L^2}{\rho\nu^2Gr_L}(\bar{p},\bar{p}_p)\\ (v,v_p)=\frac{\rho L}{\mu}Gr_L^{-1/4}\left((\bar{v},\bar{v}_p)-\sigma_x(\bar{u},\bar{u}_p)\right),\ a=\frac{\bar{a}}{L}\\ \sigma_x=\frac{d\bar{\sigma}}{d\bar{x}}=\frac{d\sigma}{dx},\ \sigma(x)=\frac{\sigma(\bar{x})}{L},\ Gr_L=\frac{g\beta_TT_0L^3}{\nu^2},\\ \nu=\frac{\mu}{\rho},\ \mathrm{Pr}=\frac{\nu}{\alpha}\end{array}\tag{13}$$

By incorporating Eq. (13), the dimensional continuity, momentum and temperature equations for both phases will be transformed in underlying form.
For the gas phase:

$$\frac{\partial u}{\partial x}+\frac{\partial v}{\partial y}=0\tag{14}$$

$$u\frac{\partial u}{\partial x}+v\frac{\partial u}{\partial y}=-\frac{\partial p}{\partial x}+\sigma_xGr_L^{1/4}\frac{\partial p}{\partial y}+\left(1+\sigma_x^2\right)\frac{\partial^2u}{\partial y^2}+\theta+D_\rho\alpha_d(u_p-u)\tag{15}$$

$$\sigma_x\left(u\frac{\partial u}{\partial x}+v\frac{\partial u}{\partial y}\right)+\sigma_{xx}u^2=-Gr_L^{1/4}\frac{\partial p}{\partial y}+\sigma_x\left(1+\sigma_x^2\right)\frac{\partial^2u}{\partial y^2}+\sigma_xD_\rho\alpha_d(u_p-u)\tag{16}$$

$$u\frac{\partial\theta}{\partial x}+v\frac{\partial\theta}{\partial y}=\frac{1}{\mathrm{Pr}}\left(1+\sigma_x^2\right)\frac{\partial^2\theta}{\partial y^2}+\frac{2}{3\mathrm{Pr}}D_\rho\alpha_d(\theta_p-\theta)\tag{17}$$

For the particle phase:

$$\frac{\partial u_p}{\partial x}+\frac{\partial v_p}{\partial y}=0\tag{18}$$

$$u_p\frac{\partial u_p}{\partial x}+v_p\frac{\partial u_p}{\partial y}=-\frac{\partial p_p}{\partial x}+\sigma_xGr_L^{1/4}\frac{\partial p_p}{\partial y}-\alpha_d(u_p-u)\tag{19}$$

$$\begin{array}{l}\sigma_x\left(u_p\frac{\partial u_p}{\partial x}+v_p\frac{\partial u_p}{\partial y}\right)+u_p^2\sigma_{xx}\\ \quad=-Gr_L^{1/4}\frac{\partial p_p}{\partial y}-\alpha_d\sigma_x(u_p-u)\end{array}\tag{20}$$

$$u_p\frac{\partial\theta_p}{\partial x}+v_p\frac{\partial\theta_p}{\partial y}=-\frac{2}{3\gamma\mathrm{Pr}}\alpha_d(\theta_p-\theta)\tag{21}$$

The corresponding boundary conditions for gas and particle phase becomes:
For gas phase:

$$\begin{gathered}\frac{\partial u}{\partial y}(x,0) = -\lambda\frac{\partial \theta}{\partial x}(x,0), v(x,0) = 0, \theta(x,0) = 1 \\ u(x,\infty) = 0, \theta(x,\infty) = 0.\end{gathered} \tag{22}$$

For particle phase:

$$\begin{gathered}\frac{\partial u_p}{\partial y}(x,0) = -\lambda\frac{\partial \theta_p}{\partial x}(x,0), v_p(x,0) = 0, \theta_p(x,0) = 1 \\ u_p(x,\infty) = 0, \theta_p(x,\infty) = 0.\end{gathered} \tag{23}$$

where, $\lambda = Ma/Gr_L^{3/4}$ is a function of Marangoni number and Ma takes the form as: $Ma = \hbar_T T_0 L/\mu\nu$. The dimensionless mathematical expressions for the interaction of two-phases are gives as:

$$\gamma = \frac{c_s}{c_p}, \quad \tau_T = \frac{3}{2}\gamma\tau_m \mathrm{Pr}, \quad D_\rho = \frac{\rho_p}{\rho}, \quad \alpha_d = \frac{L^2}{\tau_m \nu Gr_L^{1/2}} \tag{24}$$

where, γ, D_ρ, α_d are respectively symbolizing the specific heat ratio of the mixture, mass concentration of particle phase and the dust parameter. It is important to mention here that for different mixtures, the interaction term γ may vary between 0.1 and 10.0 (For details see [16]). It can also be observed that for $\alpha_d = 0.0$, the flow governs by the natural convection in the absence of the dusty particles (i.e carrier phase only). Further, the Eqs. (15) and (19) respectively indicate that the pressure gradient of the gas and the particle phase along the y direction are of $O(Gr^{-1/4})$, which implies that the lowest order pressure gradient of both phases along the x direction can be determined from the inviscid-flow solution. In the present problem, this pressure gradient is zero because there is no externally induced free stream. Moreover, Eq. (15) shows that $Gr^{1/4}\partial p/\partial y$ is of O(1) and can be determined by the left-hand side of this equation. Thus, the elimination of $\partial p/\partial y$ from Eqs. (15) and (16) leads to:

$$u\frac{\partial u}{\partial x} + v\frac{\partial u}{\partial y} + \frac{\sigma_x \sigma_{xx}}{(1+\sigma_x^2)}u^2 = \left(1+\sigma_x^2\right)\frac{\partial^2 u}{\partial y^2} + \frac{\theta}{(1+\sigma_x^2)} + D_\rho \alpha_d \left(u_p - u\right) \tag{25}$$

On the similar lines, removal of $\partial p_p/\partial y$ from Eqs. (19) and (20) results into:

$$u_p\frac{\partial u_p}{\partial x} + v_p\frac{\partial u_p}{\partial y} + \frac{\sigma_x \sigma_{xx}}{(1+\sigma_x^2)}u_p^2 = -D_\rho \alpha_d \left(u_p - u\right) \tag{26}$$

Now, for numerical treatment for the present problem, we have employed the implicit finite difference (Thomas Algorithm). For this, first we introduce the following transformations to reduce the system of boundary layer equations into some convenient form:

$$\begin{aligned}&x = X, \quad y = x^{\frac{1}{4}}Y, \ (u, u_p) = x^{\frac{1}{2}}(U, U_p), \\ &(v, v_p) = x^{-\frac{1}{4}}(V, V_p), \ (\theta, \theta_p) = (\Theta, \Theta_p)\end{aligned} \tag{27}$$

By incorporating the transformation defined in Eq. (27), the above system of dimensionless boundary layer equations can be further mapped into the non-conserved form as follows:
For gas phase:

$$\frac{1}{2}U + X\frac{\partial U}{\partial X} - \frac{1}{4}Y\frac{\partial U}{\partial Y} + \frac{\partial V}{\partial Y} = 0 \tag{28}$$

$$\left(\frac{1}{2}+\frac{X\sigma_X\sigma_{XX}}{\left(1+\sigma_X^2\right)}\right)U^2+XU\frac{\partial U}{\partial X}+\left(V-\frac{1}{4}YU\right)\frac{\partial U}{\partial Y}=\left(1+\sigma_X^2\right)\frac{\partial^2 U}{\partial Y^2} +\frac{\Theta}{\left(1+\sigma_X^2\right)}+D_\rho\alpha_d X^{1/2}(U_p-U) \tag{29}$$

$$XU\frac{\partial\Theta}{\partial X}+\left(V-\frac{1}{4}YU\right)\frac{\partial\Theta}{\partial Y}=\frac{\left(1+\sigma_X^2\right)}{\mathrm{Pr}}\frac{\partial^2\Theta}{\partial Y^2}+\frac{2}{3\mathrm{Pr}}D_\rho\alpha_d X^{1/2}\left(\Theta_p-\Theta\right) \tag{30}$$

$$\frac{1}{2}U_p+X\frac{\partial U_p}{\partial X}-\frac{1}{4}Y\frac{\partial U_p}{\partial Y}+\frac{\partial V_p}{\partial Y}=0 \tag{31}$$

$$\left(\frac{1}{2}+\frac{X\sigma_X\sigma_{XX}}{\left(1+\sigma_X^2\right)}\right)U_p^2+XU_p\frac{\partial U_p}{\partial X}+\left(V_p-\frac{1}{4}YU_p\right)\frac{\partial U_p}{\partial Y}=-\alpha_d X^{1/2}(U_p-U) \tag{32}$$

$$XU_p\frac{\partial\Theta_p}{\partial X}+\left(V_p-\frac{1}{4}YU_p\right)\frac{\partial\Theta_p}{\partial Y}=-\frac{2}{3\gamma\mathrm{Pr}}\alpha_d X^{1/2}\left(\Theta_p-\Theta\right) \tag{33}$$

The transformed boundary conditions can be written as:
For gas phase:

$$\begin{array}{c}\frac{\partial U}{\partial Y}(X,0)=-\lambda X^{-1/4}\frac{\partial\Theta}{\partial X}(X,0), V(X,0)=0,\\ \Theta(X,0)=1, U(X,\infty)=0, \Theta(X,\infty)=0.\end{array} \tag{34}$$

For particle phase:

$$\begin{array}{c}\frac{\partial U_p}{\partial Y}(X,0)=-\lambda X^{-1/4}\frac{\partial\Theta_p}{\partial X}(X,0), V_p(X,0)=0,\\ \Theta_p(X,0)=1, U_p(X,\infty)=0, \Theta_p(X,\infty)=0.\end{array} \tag{35}$$

A numerical solution for the coupled system of non linear partial differential Eqs. (28)-(35) by a finite difference method is straightforward, since the computational grids can be fitted to the body shape in (X,Y) coordinates. The discretization process is carried out by exploiting the central difference quotients for diffusion terms, and the forward difference for the convection terms. The computational process is started at $X=0.01$ as the singularity at this point has been removed by the scaling. At every X station, the computations are iterated until the difference of the results, of two successive iterations become less or equal to 10^{-6}. In order to get accurate results, we have compared the results at different grid size in Y direction and reached at the conclusion to chose $\Delta Y=0.003$. In this integration, the maximum value of Y is taken to be 30.0. A detail description of discretization procedure and numerical scheme is presented in [32].
The measurable physical quantities like local skin friction coefficient, τ_w, and rate of heat transfer, Q_w, are used to express the solutions of the current scenario. These quantities are much significant from an engineering point of view, as both can be served to improve many equipments in aerodynamics. After some algebraic manipulations, the dimensionless expressions for skin friction coefficient and heat transfer rate are obtained as:

$$\begin{aligned}\tau_w&=C_f\left(\frac{Gr^{-3}}{X}\right)^{1/4}=\sqrt{1+\sigma_X^2}\left(\frac{\partial U}{\partial Y}\right)_{Y=0}\\ Q_w&=Nu\left(\frac{Gr}{X}\right)^{-1/4}=-\sqrt{1+\sigma_X^2}\left(\frac{\partial\Theta}{\partial Y}\right)_{Y=0}\end{aligned} \tag{36}$$

In the upcoming section, the obtained results are graphed and discussed.

3 Results and Discussion

The main purpose of present analysis is to investigate the effects of thermal Maragoni convection on two-phase dusty fluid flow past a vertical wavy surface. We performed two-dimensional simulations in order to obtain solutions of mathematical model presented in terms of primitive variables given in Eqs. (28)-(35) from the two-point implicit finite difference method. Numerical results are reported for the overall effectiveness of mass concentration of dust particles in fluid which is moving along a transverse geometry. Particularly, the solutions are established for the water particulate suspension (i.e, Pr = 7.0, $D_\rho = 10.0$ and $\gamma = 0.1$). The parametric values for dusty water are taken from study of Apazidis [33]. While the numerical computations are performed by setting the values of other parameters as: $\lambda = 1.0$, $\alpha_d = 0.1, 0.5, 1.0$ and $a = 0.3, 0.4, 0.5$. The numerical values of τ_w and Q_w for clear and dusty fluid are entered in Table 1. It is important to mention here that, $D_\rho = 0.0$, recovers the model for one phase flow. The quantitative data clearly shows the influence of mass concentration of dust particle parameter on the skin friction and rate of heat transfer. The data for τ_w and Q_w indicates that the both physical quantities are maximum for clear fluid and reduces due to the increment in values of particle loading parameter D_ρ.

Graphical presentation of τ_w and Q_w is given in Fig. 2 for water particle mixture. For

Table 1: Numerical values of τ_w and Q_w for $D_\rho = 0.0, 5.0$, Pr = 0.7, $\gamma = 0.1$, $\alpha_d = 0.1$, $\lambda = 1.0$ and $a = 0.3$.

X	τ_w		Q_w	
	$D_\rho =$ 0.0	$D_\rho =$ 5.0	$D_\rho =$ 0.0	$D_\rho =$ 5.0
0.01999	0.00168	0.00162	0.93411	0.90981
1.00900	0.00189	0.00162	1.03399	0.93683
2.00800	0.00202	0.00170	1.03882	0.93766
3.00700	0.00210	0.00177	1.03478	0.93366
4.00600	0.00217	0.00183	1.02852	0.92861
5.00500	0.00224	0.00190	1.02153	0.92337
6.00400	0.00230	0.00196	1.01432	0.91823
7.00300	0.00236	0.00203	1.00711	0.91330
8.00200	0.00242	0.00211	1.00001	0.90863
9.00100	0.00248	0.00218	0.99307	0.90425
10.0000	0.00255	0.00226	0.98634	0.90016

comparison, skin friction coefficient and rate of heat transfer are plotted for the suspension without dust particles (clear fluid). In Fig. 2, it can be seen that both the skin friction coefficient and rate of heat transfer decreases by increasing the value of mass concentration parameter D_ρ. Such behavior is expected because the carrier fluid loses the kinetic and thermal energy by interacting with the dust particles and this leads to decrease the velocity of carrier fluid as compared to pure fluid case. Ultimately the velocity gradient for the carrier fluid decreases at the surface of the wavy plate. Particularly, It can be seen from Fig. 2(b) that the rate of heat transfer shows a considerable decline by increasing the mass concentration parameter, D_ρ, for water particulate suspension. Therefore, it happened subject to the interaction of the two phase flow.

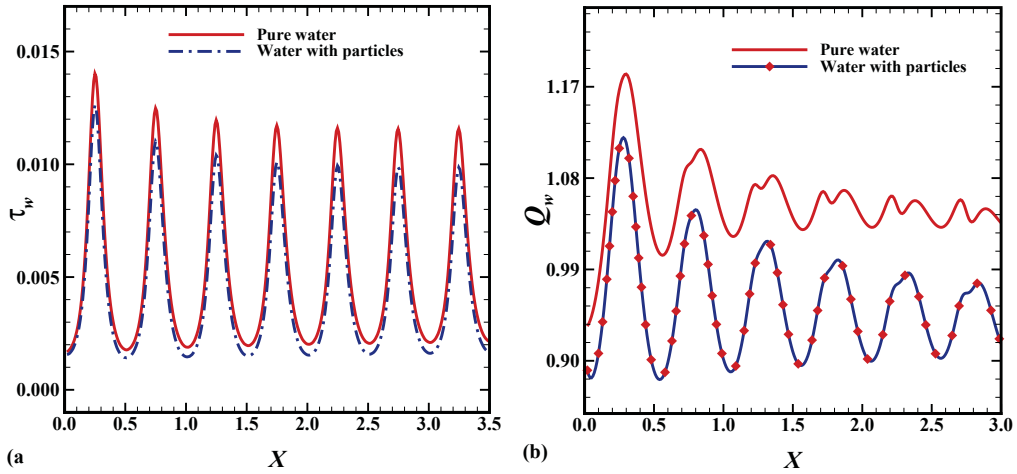

Fig. 2(a) Skin friction and (b) Rate of heat transfer for $D_\rho = 0.0, 10.0$ **while** $\mathbf{Pr} = 7.0$, $\gamma = 0.1$, $\alpha_d = 0.1$, $\lambda = 1.0$ **and** $a = 0.3$.

Fig. 3 is plotted to visualize the effect of amplitude of wavy surface on the distribution of physical quantities, namely, τ_w and Q_w. The change in surface contour is followed by raise and fall of the curves. As it can be visualize from Fig. 3(a), that the influence of amplitude a, on average, is to reduce the rate of skin friction. Similar behavior is recorded for the rate of heat transfer (see Fig. 3(b)). As a whole, the rate of heat transfer, Q_w, reduces when the amplitude of the sinusoidal waveform increases. As the amplitude increases the shape of the wave gradually changes from sinusoidal waveform to the unusual shape. The reduction in the magnitude of the temperature gradient happened due to the simultaneous influence of centrifugal and buoyancy force. Furthermore, we notice that the change in rate of heat transfer is more pronounced for larger values of the amplitude a and this factor acts as a retarding force for heat transfer coefficient.

Fig. 4 displays the variation in quantities: τ_w and Q_w that are brought by changing the value of dust parameter (α_d) of the water suspension. It is interesting to infer from this figure that the skin friction coefficient remains insensitive but rate of heat transfer shows reduction within the boundary layer region when α_d increases. The presence of inert particles in water are responsible for reduction of Q_w. Higher the value of dust parameter, smaller will be the rate of heat transfer. As observed from the expression of α_d that dust parameter is inversely proportional to the velocity relaxation time (τ_m). Therefore, for $\tau_m >> 1$ the dust parameter will be small, i.e., $\alpha_d << 1$, on the other hand, for $\tau_m << 1$ the dust parameter must be large enough. Keeping this in mind, the numerical results displayed in Fig. 4 ranges from 0.1 to 5.0.

Fig. 5 is plotted to visualize the detailed scenario of velocity and temperature profiles of carrier and particle phases for various values of amplitude of wavy surface a. As it can clearly seen form Fig. 5(a), that the velocities for both phases decreases significantly owing to increase in value of amplitude a. Such behavior is expected, because when amplitude of the wavy surface increases, the water particulate suspension between crust and trough of the waves undergoes more resistance to flow and hence fluid velocity decreases. As, small values of a offers no resistance to flow and suspension quickly attains its asymptotic value

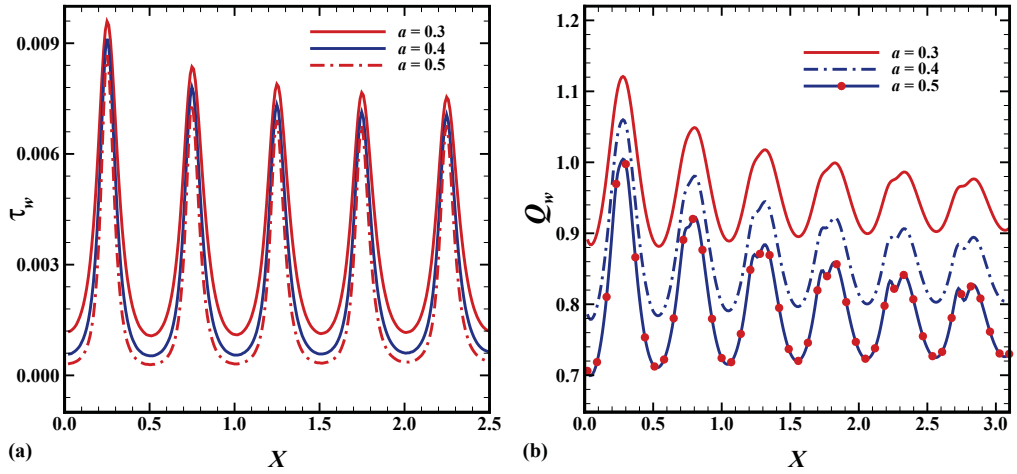

Fig. 3(a) Skin friction and (b) Rate of heat transfer for $a = 0.3, 0.4, 0.5$ while Pr $= 7.0$, $D_\rho = 10.0$, $\gamma = 0.1$, $\alpha_d = 0.1$ and $\lambda = 1.0$.

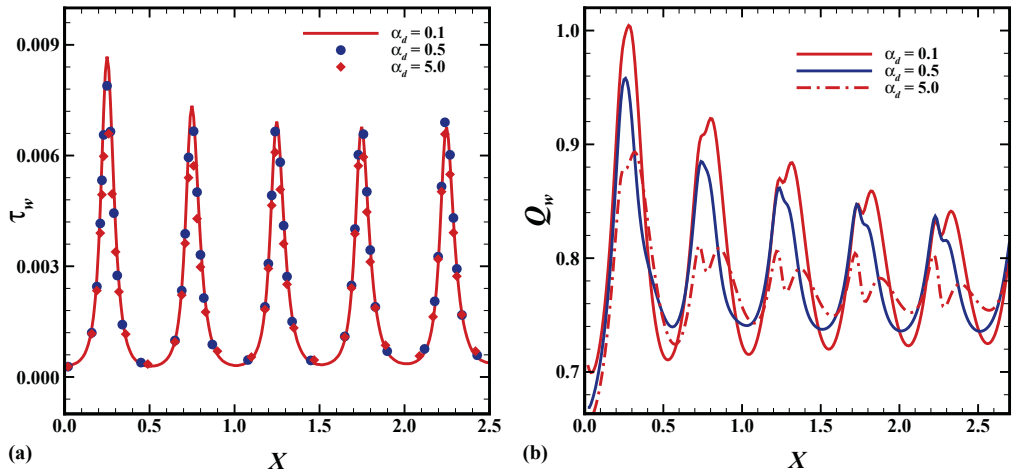

Fig. 4(a) Skin friction and (b) Rate of heat transfer for $\alpha_d = 0.1, 1.0, 5.0$ while Pr $= 7.0$, $D_\rho = 10.0$, $\gamma = 0.1$, $\lambda = 1.0$ and $a = 0.5$.

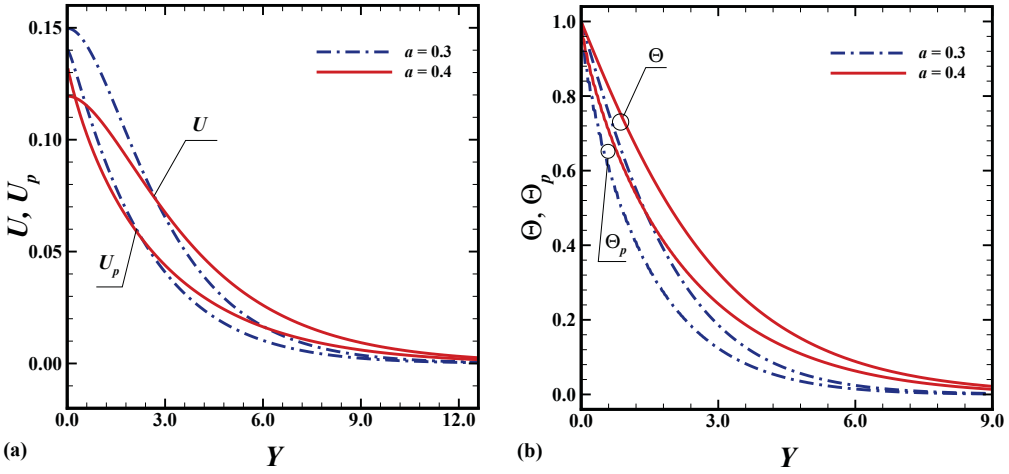

Fig. 5(a) Velocity and (b) Temperature profiles for $a = 0.3, 0.4$ **while Pr** $= 7.0$**,** $D_\rho = 10.0$**,** $\gamma = 0.1$**,** $\alpha_d = 0.1$**,** $\lambda = 1.0$ **and** $X = 10.0$**.**

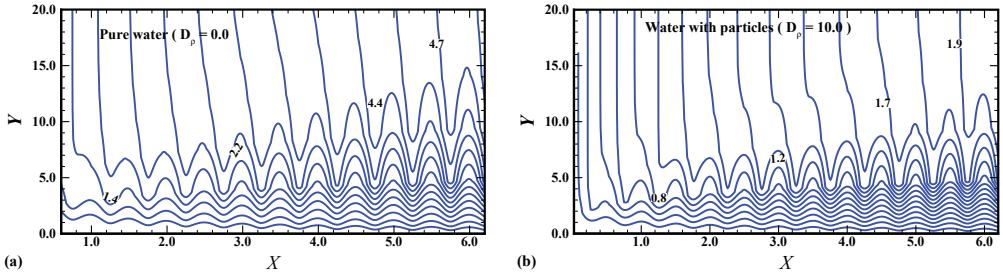

Fig. 6 Streamlines for (a) $D_\rho = 0.0$**, (b)** $D_\rho = 10.0$ **for Pr** $= 7.0$**,** $\gamma = 0.1$**,** $\alpha_d = 0.1$**,** $\lambda = 1.0$ **and** $a = 0.3$**.**

in the boundary layer region. However, the parameter a has reverse affect on temperature profile (see Fig. 5(b)). This may happens due to the fact that, the dust particles near the surface attains the thermal energy from the hotter surface of large amplitude and ultimately give rise to the temperature of dusty fluid in whole convective regime.

In order to illustrate the influence of mass concentration of dust particles parameter, D_ρ on streamlines and isotherms for water particulate suspension, Figs. 6 and 7 are plotted. For comparison, suspension without particle cloud (pure water) is also presented in Figs. 6(a) and 7(a). It is observed that by loading the dust particles, the velocity and the temperature of dusty fluid reduces significantly as compared to clear fluid (pure water) as shown in Fig. 6(a) and 7(a). When particles are loaded extensively, (i.e, $D_\rho = 10.0$), the base fluid loses the kinetic and thermal energy due to inter-collisions of particles, which ultimately decrease the overall velocity and temperature into the boundary layer region.

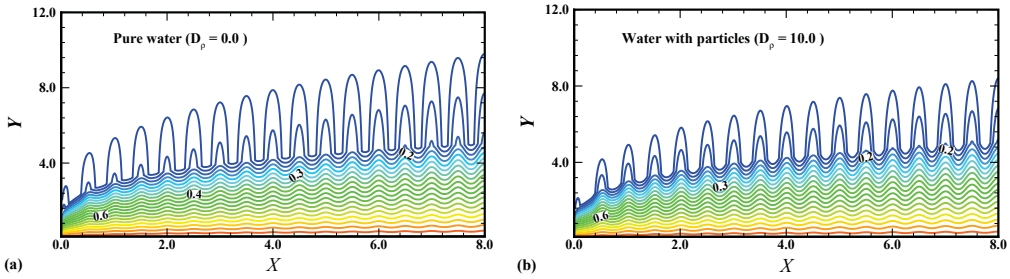

Fig. 7 Isotherms for (a) $D_\rho = 0.0$, (b) $D_\rho = 10.0$ for Pr $= 7.0$, $\gamma = 0.1$, $\alpha_d = 0.1$, $\lambda = 1.0$ and $a = 0.3$.

4 Conclusion

In this study, detailed numerical solutions are obtained for thermal Maragoni convection of two phase dusty boundary layer flow, induced by the semi-infinite vertical wavy surface. Coordinate transformations (primitive variable formulations) are applied to switch the governing equations of the carrier and the dispersed phase into another set of equations. Two-point finite difference solutions are obtained for the whole length of the irregular surface. The focus of this study is to analyze the behavior of thermal Maragoni convection on dusty fluid flow along an uneven surface. Effect of various emerging parameters are explored by expressing their relevance on skin friction coefficient and rate of heat transfer. Numerical results give a clear insight towards understanding the response of the present physical situation. Velocity and temperature distributions are plotted and visualized as well through streamlines and isotherms. From this analysis, it is observed that mass concentration parameter and amplitude of wavy surface parameter reduces the rate of heat transfer within the boundary layer region.

References

[1] Napolitano, L. G., Microgravity fluid dynamics, In:2nd Levitch conference, Fluid Sciences under Microgravity, Washington, ESA SP-295, 1978, 47-58.

[2] Napolitano, L. G., Marangoni boundary layers, In: Proceedings of the 3rd European symposium on material science in space, Grenoble, ESA SP-142, 1979.

[3] Drezet, J. M., Pellerin, S., Bezencon, C., Mokadem, S., Modelling the Marangoni convection in laser heat treatment, *J. Phys. France*, **120**, 2004, 299-306.

[4] Skarda, J. R. L., Jacqmin, D. Mccaughan, F. E., Exact and approximate solutions to the double diffusive Marangoni-Bènard problem with cross-diffusive terms, *J. Fluid Mech.*, **366**, 1998, 109-133.

[5] Batishchev, V. A., Kuznetsov, V. V., Pukhnachev, V. V., Marangoni boundary layers, *Prog. Aerosp. Sci.*, **26**, 1989, 353-370.

[6] Napolitano, L. G., Russo, G., Similar axially symmetric Marangoni boundary layers, *Acta Astronautica*, **11**, 1984, 189-198.

[7] Napolitano, L. G., Surface and buoyancy driven free convection, *Acta Astronautica*, **9**, 1982, 199-215.

[8] Napolitano, L. G., Golia, C., Coupled Marangoni boundary layers, *Acta Astronautica*, **8**, 1981, 417-434.

[9] Christopher, D. M., Wang, B., Prandtl number effects for Marangoni convection over a flat surface, *Int. J. Therm. Sci.*, **40**, 2001, 564-570.

[10] Golia, C., Viviani, A., Non isobaric boundary layers related to Marangoni flows, *Meccanica*, **21**, 1986, 200-204.

[11] Pop, I., Postelnicu, A., Grosan, T., Thermosolutal Marangoni forced convection boundary layers, *Meccanica*, **36**, 2001, 555-571.

[12] Al-Mudhaf, A. Chamkha, A. J., Similarity solutions for MHD thermosolutal Marangoni convection over a flat surface in the presence of heat generation or absorption effects, *Heat and Mass Transfer*, **42**, 2005, 112-121.

[13] Magyari, E., Chamkha, A. J., Exact analytical solutions for thermosolutal Marangoni convection in the presence of heat and mass generation or consumption, *Heat and Mass Transfer*, **43**, 2007, 965-974.

[14] Magyari, E. Chamkha, A. J., Exact analytical results for the thermosolutal MHD Marangoni boundary layer, *Int. J.Thermal Sci.*, **47**, 2008, 848-857.

[15] Zueco, J., Bèg, O. A., Network numerical simulation of hydromagnetic Marangoni mixed convection boundary layers, *Chemical Eng. Commun.*, **198**, 2011, 552-571.

[16] Rudinger, G., Fundamentals of gas-particle flow, Elsevier Scientific Publishing Co., Amsterdam, 1980.

[17] Farbar, L., Morley, M. J., Heat transfer to flowing gas-solid mixtures in a circular tube, *Ind. Eng. Chem.*, **49**, 1957, 1143-1150.

[18] Marble, F. E., Dynamics of a gas containing small solid particles, combustion and propulsion, 5th AGARD colloquium, Pergamon press, 1963.

[19] Singleton, R. E., Fluid mechanics of gas-solid particle flow in boundary layers, Ph.D. Thesis, California Institute of Technology, 1964.

[20] Michael, D. H., Miller, D. A., Plane parallel flow of a dusty gas, *Mathematica*, **13**, 1966, 97-109.

[21] Saffman, P. G., On the stability of laminar flow of a dusty gas, *J. Fluid Mech.*, **13**, 1962, 120-128.

[22] Siddiqa, S., Hossain, M. A., Saha, S. C., Two-phase natural convection flow of a dusty fluid, *Int. J. Numer. Method*, **25**, 2015, 1542- 1556.

[23] Siddiqa, S., Begum, N., Hossain, M. A., Gorla, R. S. R., Numerical solutions of natural convection flow of a dusty nanofluid about a vertical wavy truncated cone, *J. Heat Transfer*, **139**, 2017, [DOI:10.1115/1.4034815].

[24] Siddiqa, S., Begum, N., Hossain, M. A., Mustafa, N., Gorla, R. S. R., Two-phase dusty fluid flow along a cone with variable properties, *Heat Mass Transfer*, [DOI: 10.1007/s00231-016-1918-y].

[25] Siddiqa, S., Begum, N., Hossain, M. A., Massarotti, N., Influence of thermal radiation on contaminated air and water flow past a vertical wavy frustum of a cone, *Int. commun. Heat Mass Transfer*, **76**, 2016, 63-68.

[26] Yao, L. S., Natural convection along a vertical wavy surface, *J. Heat Transfer*, **105**, 1983, 465-468.

[27] Moulic, S. G., Yao, L. S., Natural convection along a wavy surface with uniform heat flux, *J. Heat Transfer*, **111**, 1989, 1106-1108.

[28] Rees, D. A. S., Pop, I., Free convection induced by a vertical wavy surface with uniform heat flux in a porous medium, *J. Heat Transfer*, **117**, 1995, 545-550.

[29] Molla, M. M., Hossain, M. A., Gorla, R. S. R., Radiation effects on natural convection boundary layer flow over a vertical wavy frustum of a cone, *Proc. IMechE Part C: J. Mechanical Engineering Science*, **223**, 2009 1605-1614.

[30] Siddiqa, S., Begum, N., Hossain, M. A., Compressible dusty gas along a vertical wavy surface, *Appl. Math. Comput.*, **293**, 2017, 600-610.

[31] Siddiqa, S., Hina, G., Begum, N., Hossain, M. A., Gorla, R. S. R., Numerical solutions of nanofluid bioconvection due to gyrotactic microorganisms along a vertical wavy cone, *Int. J. Heat Mass Transfer*, **101**, 2016, 608-613.

[32] Siddiqa, S., Begum, N., Hossain, M. A., Radiation effects from an isothermal vertical wavy cone with variable fluid properties, *Appl. Math. Comput.*, **289**, 2016, 149-158.

[33] Apazidis, N., Temperature distribution and heat transfer in a particle-fluid flow past a heated horizontal plate, *Int. J. Multiphase Flow*, **16**, 1990, 495-513.